AGU ADVANCING EARTH AND SPACE SCIENCE

Geophysical Research Letters®

RESEARCH LETTER
10.1029/2021GL096376

Supernova Rates and Burial of Organic Matter

Henrik Svensmark[1]

[1]National Space Institute, Technical University of Denmark, Lyngby, Denmark

Key Points:

- The fraction of organic carbon buried in marine sediments covaries with changes in supernova frequency over most of the Earth's history
- Supernovae influence Earth via a link between atmospheric ionization, clouds and climate. High cosmic ray flux leads to a cold climate
- Climatic induced ocean circulation regulates nutrients to the biosphere. A larger bioproductivity results in increased organic matter burial

Supporting Information:

Supporting Information may be found in the online version of this article.

Correspondence to:

H. Svensmark,
hsv@space.dtu.dk

Citation:

Svensmark, H. (2021). Supernova rates and burial of organic matter. *Geophysical Research Letters*, *48*, e2021GL096376. https://doi.org/10.1029/2021GL096376

Received 1 OCT 2021
Accepted 12 DEC 2021

Abstract Life on Earth appears to have evolved under the influence of supernovae activity in the solar neighborhood. Supernovae frequency regulates the flux of cosmic ray particles arriving at the top of the Earth's atmosphere, where empirical evidence supports a close connection between cosmic rays, clouds, and climate. Burial of organic matter in marine sediments follows cosmic rays variations for more than 3.5 Gyr and in detail during the last 500 Myr. The supernovae link to the burial of organic matter may be due to climate-induced changes in the atmospheric and oceanic circulation affecting the availability of nutrients and the bioproductivity in the oceans. A higher bioproductivity then leads to a more extensive burial of organic matter. Support for this scenario comes from a proxy of nutrient concentrations in the ocean which covaries with the supernovae frequency. The results suggest a fundamental connection between supernovae rates and life on Earth.

Plain Language Summary The study proposes a surprising link between the burial of organic matter in sediments and stellar processes. The paper has two components; the first component concerns empirical evidence: A close correlation between the fraction of organic matter buried in sediments and changes in supernovae frequency. This correlation is evident during the last 3.5 billion years (see Figure 2) and in close detail over the previous 500 Myr (see Figure 4). All astrophysical data, for example, changes in star formation and the inferred changes in supernovae frequency, are based on peer-reviewed works, as is the carbon 13 data. The second component of the paper gives a possible justification for the observed correlations. The assumption is that changes in supernovae frequency result in climate change, which changes the mixing in oceans and river runoff and ultimately influences nutrient availability—a high nutrient concentration results in a larger bioproductivity and a larger burial of organic matter in sediments. Again empirical evidence for this connection comes from concentrations of trace elements in pyrite (a proxy of ocean nutrient concentrations) which correlate with supernovae frequency changes over the previous 500 Myr (see Figure 5).

1. Introduction

That life on Earth has constantly been subject to strong environmental changes has been among the major revelations from geology. Events such as climate changes, sea-level changes, anoxic events, major volcanic eruptions, large impacts, and plate tectonic activity have been suggested as significant elements in the evolution of life (Cañón-Tapia & Walker, 2004; Hallam & Wignall, 1997; House, 2002; Keller, 2005; Racki, 2005; Rich et al., 1986; Smith & Pickering, 2003; Walliser, 1996).

Here, I will show a remarkable correlation between changes in star-formation in the solar neighborhood and the burial of organic matter in marine sediment. Star formation is just the first part of a chain that ends with a climatic impact on the environmental conditions life has to endure (Isozaki, 2019; Shaviv, 2002, 2003; Shaviv & Veizer, 2004). Star formation leads to short-lived massive stars that end as core-collapse supernovae. Such events make shock fronts in the interstellar medium, accelerating atomic nuclei (~90% protons) to very high energies. This particle flux, called galactic cosmic rays (GCRs), fills the interstellar medium. A fraction enters the solar system and ends up in Earth's atmosphere, becoming the primary source of atmospheric ionization. Then, the idea is that atmospheric ionization modulates the formation of cloud-condensation-nuclei and thereby cloudiness and, ultimately, Earth's energy budget. A high cosmic ray flux results in increased cloudiness and a colder climate (Svensmark, 1998; Svensmark & Friis-Christensen, 1997; H. Svensmark et al., 2007, 2013, 2017, 2021).

Progress has been made in understanding the link between atmospheric ionization by GCR, clouds, and climate. Studies have demonstrated that ions influence the formation of new aerosols (Kirkby et al., 2011; H. Svensmark et al., 2007) and aerosol growth (H. Svensmark et al., 2017), whereby they regulate the number of aerosols surviving to form cloud condensation nuclei (CCN). The number of CCN's are essential for cloud microphysics, for example, the cloud lifetime and thereby the cloud fraction. Since clouds can regulate the solar

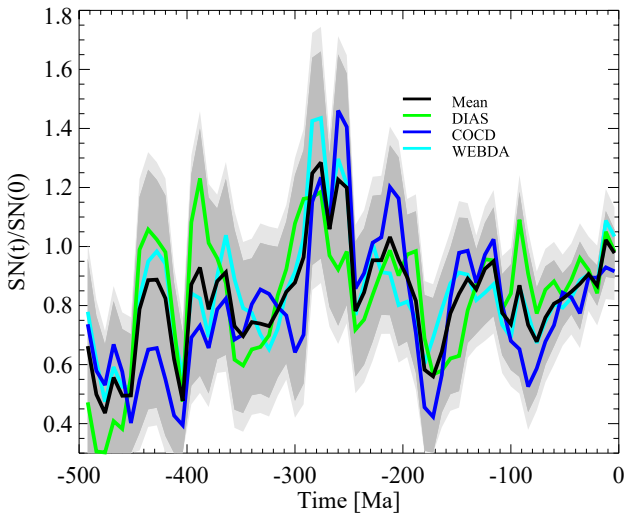

Figure 1. Variation in relative supernova frequency using three open cluster catalogs. WEBDA catalog (273 clusters with distance from solar system ≤850 pc and age ≤500 Myr) (cyan curve). The green curve is the Dias et al. (2010) catalog (224 clusters with distance ≤850 pc and age ≤500 Myr), and finally, the blue curve is the Kharchenko et al. (2005) catalog (258 clusters with distance ≤850 pc and age ≤500 Myr). The black curve is the average of the three catalogs. The gray bands are 1σ uncertainty, random normal distribution (dark gray band), or a Poisson distribution (light gray band).

energy that can reach Earth's surface, the cosmic-ray-cloud link is important for climate. The estimated variations of 200%–300% in GCR on geological timescales will have a significant impact on the formation of atmospheric aerosols and their growth to CCN and clouds (H. Svensmark et al., 2017). More uncertain are the estimated changes in the radiative forcing for such large changes in GCR flux. It is possible to assess changes in radiative forcing during week-long decreases in cosmic rays in events called Forbush decreases. Direct measurements performed by the CERES satellite give ∼2 W/m^2 for a 15% change in GCR (H. Svensmark et al., 2021). A rough estimate of the radiative forcing for a 200%–300% change in GCR is ∼10–20 W/m^2. Such a large change is sufficient to impact climate significantly. The relevance in the present context is the remarkable correlations between changes in atmospheric GCR ionization and climate on time scales ranging from days to millions and even billions of years (Shaviv, 2002; Shaviv & Veizer, 2003, 2004; Svensmark, 1998; Svensmark, 2006a, 2012; J. Svensmark et al., 2016; Svensmark & Friis-Christensen, 1997).

If supernovae regulate climate, they also influence the circulation in the atmosphere and oceans. High levels of cosmic ray flux result in a colder climate with more extensive circulation, which provides increased nutrient flux to the biological systems and may support larger biomass and increase the fraction of biological material buried in sediments. Support for this scenario is borne out by the fraction of organic matter buried in sediments correlated closely with supernova rates over the Phanerozoic period. Simultaneously, a proxy for the concentration of nutrients in the oceans also displays a good correlation with changes in supernovae rates. Finally, since the burial of organic matter enables the accumulation of oxygen in surface environments, supernovae rates in the solar neighborhood have been vital for the evolution of life.

2. Results

2.1. Galactic Cosmic Ray Variations on Earth

There is no known geological proxy of GCR stored in sediments that can reveal variations over millions of years. Still, an alternative is to estimate the past frequency of supernovae from star formation in the solar neighborhood. The frequency of supernovae is relevant since they result in shock fronts in the interstellar media, which are the primary sources of GCR that ionize the Earth's atmosphere. Past star formation can be estimated using open stellar clusters. Open stellar clusters consist of (typically ∼10^3) stars that formed from the same gas cloud and bound together by gravity (Lada & Lada, 2003). Measurements of distance from the solar system and assessments of ages of open stellar clusters are then processed to estimate the average number of massive stars that will end as supernovae in a given age interval. This information makes it possible to infer the GCR flux on Earth (Svensmark, 2012).

Figure 1 shows as the green, cyan, and blue curve, a reconstruction of supernovae over the last 500 Myr based on three data sets of open clusters in the solar neighborhood (Dias et al., 2002; Kharchenko et al., 2005; Mermilliod, 1993) and processed as in Svensmark (2012). The difference between the various data sets (green, blue, and cyan) in Figure 1 illustrate variation caused by differences in parameters of the sampled clusters. The black curve is the mean of the three curves. The 1σ uncertainty is estimated by a bootstrap Monte Carlo method, where 37% of the cluster ages, chosen at random in a sample, are replaced by a new age. This new age is drawn from a random normal distribution (dark gray band) or a Poisson distribution (light gray band) with a 20% variance in the age and centered around the measured age and repeated for 10^3 samples.

Reaching further back in time, it gets problematic to get information on the star formation in the solar neighborhood due to orbital diffusion. Older stars close to the solar system likely originated from a torus in the Galactic disk concentric with the solar circle (The solar system orbits the Galactic center in ca. 240 Myr along a

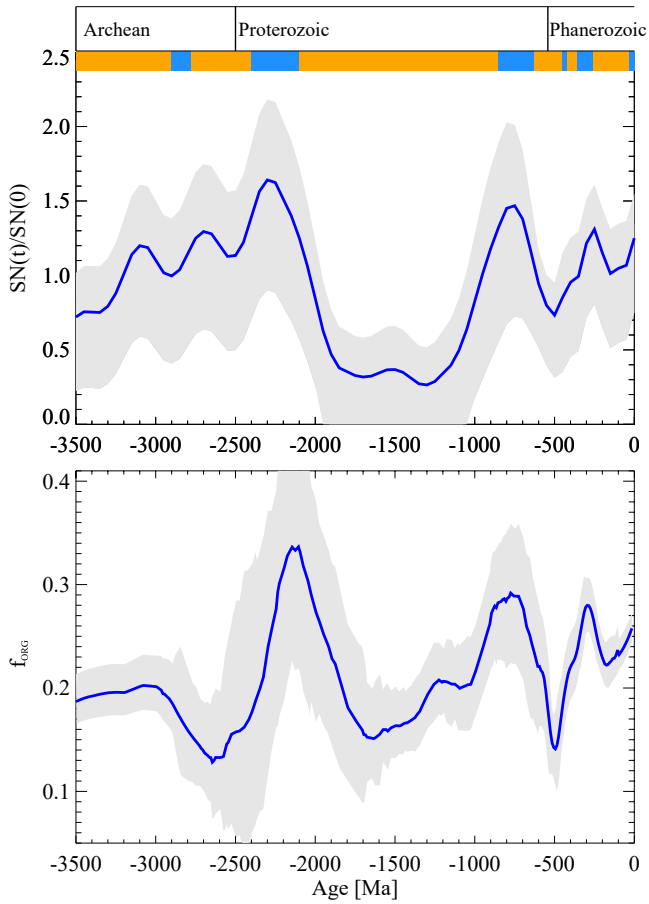

Figure 2. Top panel: Reconstructed relative cosmic ray intensity over the last 3,500 Ma. Based on star formation data Rocha-Pinto et al. (2000) and Svensmark (2006a), changes in solar evolution and open cluster data Svensmark (2012) (see text). Bottom panel: Fraction of carbon buried as organic matter in the sediments over the last 3,500 Myr reconstructed from Equation 1. The gray band is one sigma uncertainty. Colored bar at the top of figure shows major glaciations (blue) and geological time subdivision in eons.

path called the solar circle). Therefore, on time scales longer than ~500 Ma, stars in the solar neighborhood reflect bursts of star-formation along the solar circle of the Galaxy. Rocha-Pinto et al. (2000) estimates star formation based on brown dwarf stars in the solar neighborhood and covering the lifetime of the Galaxy. Using these results and correcting for solar evolution, it is possible to get a history of GCR over the lifetime of the Solar system (Svensmark, 2006a). Finally, combining the data of brown dwarf stars and the open stellar cluster data covering the last 800 Myr gives Figure 2 top panel, which is an estimate of the secular changes in GCR flux on Earth (relative to present-day values) in the last 3,500 Myr. Most notable is the large maximum at −2,300 Ma and the almost 1,000 Ma hiatus between −2,000 and −1000 Ma, followed by new maximum at −700 and −300 Ma. A burst of star-formation at −2,200 to −2,400 Ma, −550 to −770 Ma, and at −300 Ma was also noted by de la Fuente Marcos and de la Fuente Marcos (2004) and Kataoka et al. (2013). The colored bar on the top of the figure shows periods with glaciations (blue).

2.2. Galactic Cosmic Ray Variations and Climate

As an example, Figure 3 demonstrates the close correlation between variations in supernova rates and Earth climate. This figure illustrates the correspondence found over the Phanerozoic between supernova rates and Earth's climate given by changes in δ^{18}O. Gray circular points are δ^{18}O measurements, a proxy of temperature (Epstein et al., 1953), and the red dashed line is an 11 Myr average of the δ^{18}O data. Note that the δ^{18}O data was subtracted a linear trend of −8 ‰—which likely represents changes due to diagenetic re-crystallization of carbonate. Also, the δ^{18}O data were corrected for variations in ocean water pH (Royer et al., 2004; Zeebe, 1999, 2001), for details, see Supporting Information S1. One of the largest drops in supernova activity is right at the Permian-Triassic boundary ~250 Ma. One study suggests that the temperature over a short period (<4 Ma) increased dramatically from about 20–38°C at the P-Tr boundary (Sun et al., 2012), shown as the dark red curve in Figure 3. It should be noted that this large change in supernova frequency occurred at the same time as massive volcanic activity of the Siberian Traps, widely thought to be a major contributing factor to the end-Permian anoxia and mass extinction (Bond et al., 2019; Isozaki, 2019; Sial et al., 2021). The middle panel of Figure 3 shows land ice volume during glaciations. Finally, the bottom panel of Figure 3 depicts periods with large and small temperature gradients between the equator and polar regions (Boucot & Gray, 2001).

2.3. Burial of Organic Matter

A geochemical cycle fundamental for life is the carbon cycle. Due to the discrimination of ^{13}C relative to ^{12}C by photosynthesis, the isotope fractionation of δ^{13}C is a continuous biochemical record of former life processes preserved in sediments spanning almost 4 billion years (Schidlowski, 1988). I will now demonstrate a close relation between supernova rates and burial of organic matter represented by changes in δ^{13}C.

A simple model of the sources and sinks of carbon leads to an expression for the fraction f_{org} of organic matter buried in sediments (Kump & Arthur, 1999)

$$f_{\text{org}} = \frac{\delta_{in} - \delta_{carb}}{\delta_{org} - \delta_{carb}} \quad (1)$$

where the input of carbon from the mantle has $\delta_{in} = -5‰$. δ_{org} and δ_{carb} is the fractionation of organic sediments and inorganic carbonate sediments, respectively, which can be determined from measurements. *The Precambrian*

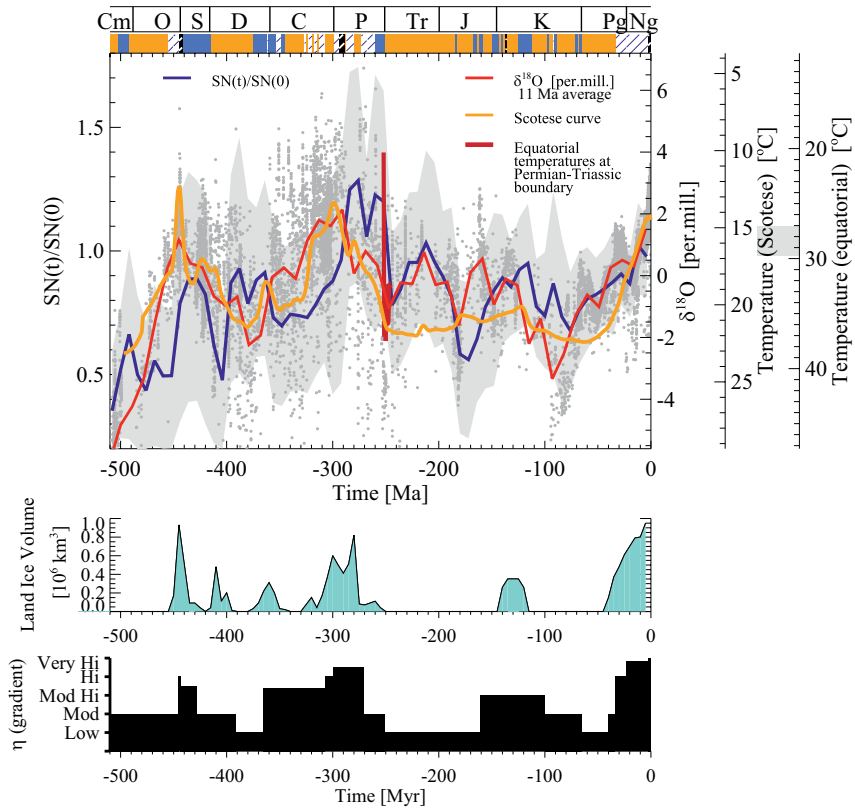

Figure 3. Variation in climate over the last 500 Myr estimated by changes in δ^{18}O, gray circular points, and an 11 Myr average (red curve), together with an estimate based on lithological data (Scotese et al. (2021), orange curve). Note that the temperature curves are inverted. The dark red curve show changes in temperature at the transition between the Permian and Triassic period (The gray bar on the right-hand scale show the present-day variations in equatorial temperatures). Note the relative good agreement with changes in supernova frequency in the solar neighborhood, blue curve, which is the mean of the three data curves in Figure 1. The gray bands are 1σ uncertainty in supernovae frequency). The colored band at the top of the figure indicates climatic warm periods (orange), cold periods (blue), glacial periods (white and blue hatched bars), and finally peak glaciations (black and white hatched bars) (Svensmark, 2012). The middle panel gives an estimate of the ice volume during glacial periods. The bottom panel is a histogram showing the evolution of the temperature gradient between polar regions and the equator based on Boucot and Gray (2001). Abbreviations for geological periods are Cm Cambrian, O Ordovician, S Silurian, D Devonian, C Carboniferous, P Permian, Tr Triassic, J Jurassic, K Cretaceous, Pg Palaeogene, Ng Neogene.

Marine Carbonate Isotope Database (Shields & Veizer, 2002), updated by Krissansen-Totton et al. (2015), provide δ^{13}C data covering the last 3.5 Ga. Measurements of δ_{carb} and δ_{org} over the last 3.5 Ga from the above database are used to construct the variation in organic and carbonate fractionation (see Figure S1 in Supporting Information S1).

From the smoothed data curves (see Figure S1 in Supporting Information S1), the burial fraction of organic matter can be reconstructed using Equation 1 and is shown in Figure 2 bottom panel. The obtained Figure 2 bottom panel is similar to the result of Bjerrum and Canfield (2004) and Krissansen-Totton et al. (2015). Note that times of maximum burial of organic matter coincide in general with glaciations in Earth climate.

The high δ^{13}C data coverage over the Phanerozoic makes it possible to show the fraction f of burial of organic matter over the last 500 Myr in further detail. Figure 4 demonstrates a clear correlation between the organic burial fraction and supernovae rates again (see figure text for data sources).

2.4. Nutrient Availability

It is possible that substantiate variations of nutrients in the ocean through geological time by measuring trace elements in marine sedimentary pyrite in black shale. Sedimentary pyrite is formed in the water column or the

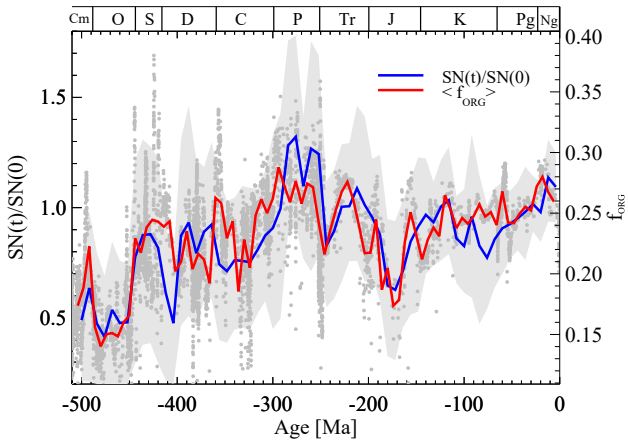

Figure 4. Changes in burial fraction *f* of organic matter over the past 500 Myr based on organic and inorganic carbon-13 in sediments (δ^{13}C in parts per mill) and shown by the scattered points, and compared here with the variations in the local supernova rates (blue curve. The gray band are 1σ uncertainty, see Figure 1). δ^{13}C in marine carbonates: Cambrian (not labeled) to Carboniferous C (Saltzman, 2005), Permian P (Grossman et al., 2008; Korte et al., 2005), Permo-Triassic transition P-Tr (Kakuwa & Matsumoto, 2006), Triassic T (Korte et al., 2005), Jurassic J to Cretaceous K (Emeis & Weissert, 2009) and Cretaceous K (Jarvis et al., 2006) and Cretaceous to present (Katz et al., 2005). Organic δ^{13}C Cambrian to Jurassic (Shields & Veizer, 2002), Jurassic J to Neogene Ng (Falkowski et al., 2005) (For a collection of δ^{13}C data see Saltzman & Thomas, 2012). The red line is a smoothing of the burial fraction. The plot starts at −510 Myr.

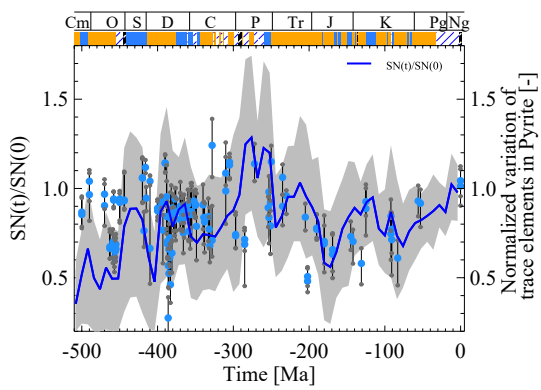

Figure 5. Average logarithmic variations of trace elements (Mn, Co, Ni, Cu, Zn, As, Se, Mo, Ag, Cd, Sb, Te, Tl, Pb, Bi) in pyrite as proxy for nutrient availability in the oceans (large blue points are average 50% percentile together with average 25% and 75% percentiles). Blue curve is the change in supernovae rate and is the mean of the three data curves in Figure 1. The gray bands are 1σ uncertainty in supernovae frequency. The colored band at the top of the figure indicates climatic warm periods (orange), cold periods (blue), glacial periods (white and blue hatched bars), and finally peak glaciations (black and white hatched bars). Abbreviations for geological periods are Cm Cambrian, O Ordovician, S Silurian, D Devonian, C Carboniferous, P Permian, Tr Triassic, J Jurassic, K Cretaceous, Pg Palaeogene, Ng Neogene.

mud at the seafloor when H_2S reacts with iron to form pyrite, FeS_2. The concentration of trace elements incorporated into sedimentary pyrite is a proxy for ocean chemistry on geological time scales (Large et al., 2014, 2015). The measured elements are Mn, Co, Ni, Cu, Zn, As, Se, Mo, Ag, Cd, Sb, Te, Tl, Pb, and Bi. Of these all, but the last four elements are known to be of importance for life. Variations in concentration through the geological time of these trace elements are a proxy of the nutrient availability (Large et al., 2015). Using two published data series (Large et al., 2014, 2015) of trace elements in pyrite from black shale over the last 500 Ma, it is possible to compare this nutrient proxy with the change in SN frequency. Figure 5 shows a normalized average logarithm variation of all the trace element concentrations plotted together with the variations in SN frequency. The logarithm concentration of each trace element-time series is subtracted from its logarithmic mean and normalized with its logarithmic variance. Then for each temporal measurement, the 25%, 50%, and 75% percentiles are found and averaged for all trace elements. In Figure 5, the large blue points averaged 50% percentile together with 25% and 75% percentiles. Note the relatively good agreement between the averaged variation in trace elements in pyrite and changes in SN frequency, which corroborates the hypothesis of a connection between SN frequency, climate, nutrient availability, and life.

3. Discussion

From Figure 1, it is seen that the relative changes in GCR flux are of the order 200%–300% in agreement with the previous estimates of Shaviv (2002) and Svensmark (2012). State-of-the-art numerical simulations of spiral arms as GCR source distributions show relative variations along the solar circle of 200%–300% consistent with the above estimate (Werner et al., 2015). However, such large changes in GCR have been questioned (Sloan & Wolfendale, 2013). For example, observations by the Fermi-satellite of diffuse gamma-radiation from proton-proton interactions in the interstellar media suggest a smaller contrast between inter-spiral-arm and spiral-arm of 20%–30%. Nevertheless, investigations of the very high-energy component of Galactic gamma rays are complicated. This complication is because the Galactic diffuse-gamma ray emission depends on several properties of the Milky Way beside the GCR source distributions, such as gas distribution, stellar radiation fields, and magnetic fields. A further complication is that Galactic diffuse-gamma ray emission data interpretation relies on numerical simulations with realistic descriptions of all the governing processes. So far, no simulation exists that meets these requirements (Werner et al., 2015).

Empirical evidence in the form of reconstructed GCR history over the last 3,500 Myr and the burial fraction of organic matter show similar variations as seen by comparing Figure 2 top panel with bottom panel. The correlation is unlikely to be accidental as testified by Figure 4, where a higher temporal resolution during the last 500 Myr shows close agreement between burial fraction and supernova history. So the question is why the supernova activity is important for the burial of organic material?

The largest bio-production in the oceans is located in the upper 200 m of the sunlit ocean mainly at the continental shelves. To maintain bio-productivity, the availability of fundamental nutrients like iron, nitrogen, phosphorus, and carbon is essential. For example, it is commonly assumed that phosphorus has been a limiting factor of bioproductivity through time (Guidry & Mackenzie, 2000). This nutrient availability must be a function of the flux into

the oceans from the land by river runoff and windblown dust. Still, important is also the ocean mixing that brings nutrients up to the surface waters (i.e., upwelling zones) along along the continental shelves. The available kinetic energy in the ocean-atmosphere system determines the mixing and transport in the oceans and atmosphere. Making the approximation that Earth is heated at the equator and cooled at the polar regions the fraction of available work, W, in the form of kinetic-energy of the circulations is in the case of an ideal Carnot cycle given by the efficiency parameter

$$\eta = \frac{W}{Q_H} = \frac{T_w - T_c}{T_w}, \tag{2}$$

where T_w and T_c are the temperature at the equator and polar regions, respectively, and Q_H is the heat put into the system. So the fraction of energy available for the mixing and circulation of nutrients is a function of the temperature difference between equator and poles. This temperature difference drives the ocean currents and winds, which in turn drives the mixing and the windblown transport of nutrients. A cold climate is characterized by a large temperature difference between poles and equator and a warm climate by a smaller temperature difference. Therefore a cold climate mixes more vigorously than a warm climate. The temperature gradient in the Cretaceous period ~100 Ma was about half of the present temperature difference. Figure 3 bottom panel illustrates the evolution of the gradient which is proportional to the efficiency parameter η in Equation 2. Note that the temporal evolution of η concurs fairly well with the supernovae frequency.

If is assumed that the net bioproductivity P is mainly limited by available nutrients and given as a balance between input of nutrients $I(\eta(t))$ and exhaustion by bioproductivity $E(P)$ as

$$\frac{dP}{dt} = I(\eta(t)) - E(P(t)). \tag{3}$$

In steady state, $dP/dt = 0$, and for linear responses, $I(\eta(t)) \propto \eta(t)$, and $E(P) \propto c_2 P$, the bioproductivity can be written as

$$P(t) \propto \eta(t) = \left(\frac{T_w - T_c}{T_w}\right) \tag{4}$$

So bioproductivity is in this picture a function of the temperature difference between the equator and poles, dictated by the delivery of nutrients by the reigning climate (Guidry & Mackenzie, 2000). An increased bioproductivity potentially gives a larger burial fraction f of organic matter in sediments (Müller & Suess, 1979). Such a scenario is in agreement with the results shown in Figure 2 top and bottom panel and in Figure 4, where supernova and burial fraction agree rather well. Ultimately, climate is affected by supernova activity, as exemplified in Figure 3, where the bottom panel shows variations in the temperature difference between the equator and polar regions.

Figure 5 shows an essential piece of evidence supporting the idea that supernovae rates couples to the nutrient availability. Here the concentrations of trace elements measured in pyrite in black shale constitute a proxy of nutrient concentrations over the Phanerozoic (Large et al., 2014, 2015). Notice the relatively good correlation between changes in supernovae frequency and the changes in trace elements. This observation supports a chain where changes in supernovae frequency affect the circulation of nutrients in the oceans and atmosphere, which is again consistent with a response in the bioproductivity manifested in the burial of organic matter, as seen in Figure 4.

Several studies support a connection between cosmic ray flux and bioproductivity by identifying a link between solar modulated cosmic rays and upwelling and bioproductivity. These studies imply high sea surface temperatures (high solar activity and lower cosmic ray flux) indicated low upwelling intensity and surface water productivity and vice versa (Munz et al., 2017; Santos et al., 2011).

The burial of organic matter is a source of oxygen in the Earth's atmosphere. The basis reaction involving oxygen is

$$6CO_2 + 6H_2O \leftrightarrow C_6H_{12}O_6(glucose) + 6O_2 \tag{5}$$

where the above reaction (left to right) represents net photosynthesis, that is, the absorption of a photon, production of oxygen, and subsequent burial of organic matter in sediments. The opposite reaction (right to left) represents the loss of oxygen by oxidation but also loss of oxygen in rock processes at high temperatures. Burial of

organic matter hinders the reaction from right to left and therefore constitutes a source of oxygen (Berner, 1989; Falkowski & Isozaki, 2008).

4. Conclusion

Empirical evidence suggests that the supernova frequency influenced the conditions for life in the oceans during most of the solar system's lifetime. It does not exclude other factors. Events like anoxic events, major volcanic eruptions, large impacts are relatively short and episodic. In contrast, changes in supernova frequency in the vicinity of the solar system are always present. The basic assumption starts with supernovae providing the particle flux that ionizes the Earth's atmosphere, which assists the formation of aerosols and cloud-condensation-nuclei, who regulate Earth's cloud cover and, thereby, climate. A high cosmic ray flux results in a colder climate. The justification for this hypothesis is experimental and observational evidence, supported here by the agreement between changes in supernovae rates and climate in the Phanerozoic.

It appears that both climate and the conditions for life have responded to the changing interstellar environment. One example presented was the fraction of carbon buried as organic matter in sediments, which reflects changes in reconstructed supernovae rates over the last 3,500 Ma. A more detailed and higher resolution time series of the burial fraction of organic matter during the Phanerozoic (last 500 Ma) also demonstrates a close correlation to supernova rates. The interpretation is that supernovae rates influence climate, which results in changes in the atmosphere-ocean circulation of nutrients. Trace elements in pyrite provide support for this picture. The concentration of trace elements in pyrite is a proxy for the ocean's nutrients, and its variation over the Phanerozoic follows the supernovae rates. Thus, nutrient concentrations control bioproductivity, and high bioproductivity results in a larger fraction of organic material buried—all in concert with the changes in supernovae rates. Oxygenic photosynthesis and organic matter burial is the primary source of oxygen, and oxygen underpins the evolution of complex life. Therefore, the evidence points to an extraordinary interconnection between life on Earth and star formation, mediated by the effect of cosmic rays on clouds and climate.

Data Availability Statement

Open Research Carbon isotope data are from: Shields and Veizer (2002); Krissansen-Totton et al. (2015). Trace elements in pyrite: Large et al. (2015).The data in Tables S1 and S2 in Supporting Information S1 are available in Svensmark, H., MNRAS, 423, 1234–1253, 397. https://doi.org/10.1111/j.1365-2966.2012.20953.x.

References

Berner, R. A. (1989). Biogeochemical cycles of carbon and sulfur and their effect on atmospheric oxygen over phanerozoic time. *Global and Planetary Change*, *1*(1), 97–122. https://doi.org/10.1016/0921-8181(89)90018-0

Bjerrum, C. J., & Canfield, D. E. (2004). New insights into the burial history of organic carbon on the early Earth. *Geochemistry, Geophysics, Geosystems*, *5*(8), Q08001. https://doi.org/10.1029/2004GC000713

Bond, D. P., Wignall, P. B., & Grasby, S. E. (2019). The Capitanian (Guadalupian, middle permian) mass extinction in NW Pangea (Borup Fiord, Arctic Canada): A global crisis driven by volcanism and anoxia. *GSA Bulletin*, *132*(5–6), 931–942. https://doi.org/10.1130/B35281.1

Boucot, A., & Gray, J. (2001). A critique of phanerozoic climatic models involving changes in the co2 content of the atmosphere. *Earth-Science Reviews*, *56*(1), 1–159. https://doi.org/10.1016/S0012-8252(01)00066-6

Cañón-Tapia, E., & Walker, G. (2004). Global aspects of volcanism: The perspectives of “plate tectonics” and “volcanic systems”. *Earth-Science Reviews*, *66*, 163–182. https://doi.org/10.1016/j.earscirev.2003.11.001

de la Fuente Marcos, R., & de la Fuente Marcos, C. (2004). On the correlation between the recent star formation rate in the Solar Neighbourhood and the glaciation period record on Earth. *New Astronomy*, *10*, 53–66. https://doi.org/10.1016/j.newast.2004.05.001

Dias, W. S., Alessi, B. S., Moitinho, A., & Lépine, J. R. D. (2002). New catalogue of optically visible open clusters and candidates. *Astronomy and Astrophysics*, *389*, 871–873. https://doi.org/10.1051/0004-6361:20020668

Dias, W. S., Alessi, B. S., Moitinho, A., & Lepine, J. R. D. (2010). Optically visible open clusters and Candidates (Dias+ 2002-2010). *VizieR Online Data Catalog*, *1*, 2022.

Emeis, K., & Weissert, H. (2009). Tethyan-Mediterranean organic carbon-rich sediments from Mesozoic black shales to sapropels. *Sedimentology*, *56*, 247–266. https://doi.org/10.1111/j.1365-3091.2008.01026.x

Epstein, S., Buchsbaum, R., Lowenstam, H. A., & Urey, H. C. (1953). Revised carbonate-water isotopic temperature scale. *GSA Bulletin*, *64*(11), 1315–1326. https://doi.org/10.1130/0016-7606(1953)64[1315:RCITS]2.0.CO;2

Falkowski, P. G., & Isozaki, Y. (2008). The story of O_2. *Science*, *322*(5901), 540–542. https://doi.org/10.1126/science.1162641

Falkowski, P. G., Katz, M. E., Milligan, A. J., Fennel, K., Cramer, B. S., Aubry, M. P., et al. (2005). The rise of oxygen over the past 205 million years and the evolution of large placental mammals. *Science*, *309*(5744), 2202–2204. https://doi.org/10.1126/science.1116047

Grossman, E. L., Yancey, T. E., Jones, T. E., Bruckschen, P., Chuvashov, B., Mazzullo, S., & sheng Mii, H. (2008). Glaciation, aridification, and carbon sequestration in the permo-carboniferous: The isotopic record from low latitudes. *Palaeogeography, Palaeoclimatology, Palaeoecology*, *268*(3–4), 222–233. https://doi.org/10.1016/j.palaeo.2008.03.053

Guidry, M., & Mackenzie, F. (2000). Apatite weathering and the phanerozoic phosphorus cycle. *Geology*, *28*. https://doi.org/10.1130/0091-7613(2000)028⟨0631:AWATPP⟩2.3.CO;2

Hallam, A., & Wignall, P. (1997). *Mass extinctions and their aftermath*. OUP Oxford. Retrieved from https://books.google.dk/books?id=M-w-CgAAQBAJ

House, M. (2002). Strength, timing, setting and cause of mid-plaeozoic extinctions. *Palaeogeography, Palaeoclimatology, Palaeoecology*, *181*, 5–25. https://doi.org/10.1016/S0031-0182(01)00471-0

Isozaki, Y. (2019). End-paleozoic mass extinction: Hierarchy of causes and a new cosmoclimatological perspective for the largest crisis. In A. Yamagishi, T. Kakegawa, & T. Usui (Eds.), *Astrobiology: From the origins of life to the search for extraterrestrial intelligence* (pp. 273–301). Springer Singapore. https://doi.org/10.1007/978-981-13-3639-3_18

Jarvis, I., Gale, A. S., Jenkyns, H. C., & Pearce, M. A. (2006). Secular variation in late cretaceous carbon isotopes: A new delta13C carbonate reference curve for the Cenomanian-Campanian (99.6-70.6 Ma). *Geological Magazine*, *143*(5), 561–608. https://doi.org/10.1017/S0016756806002421

Kakuwa, Y., & Matsumoto, R. (2006). Cerium negative anomaly just before the Permian and Triassic boundary event – The upward expansion of anoxia in the water column. *Palaeogeography, Palaeoclimatology, Palaeoecology*, *229*(4), 335–344. https://doi.org/10.1016/j.palaeo.2005.07.005

Kataoka, R., Ebisuzaki, T., Miyahara, H., & Maruyama, S. (2013). Snowball earth events driven by starbursts of the milky way galaxy. *New Astronomy*, *21*, 50–62. https://doi.org/10.1016/j.newast.2012.11.005

Katz, M. E., Wright, J. D., Miller, K. G., Cramer, B. S., Fennel, K., & Falkowski, P. G. (2005). Biological overprint of the geological carbon cycle. *Marine Geology*, *217*(3), 323–338. https://doi.org/10.1016/j.margeo.2004.08.005

Keller, G. (2005). Impacts, volcanism and mass extinction: Random coincidence or cause and effect? *Australian Journal of Earth Sciences*, *52*(4–5), 725–757. https://doi.org/10.1080/08120090500170393

Kharchenko, N. V., Piskunov, A. E., Roeser, S., Schilbach, E., & Scholz, R.-D. (2005). Catalogue of open cluster data (COCD) (Kharchenko+, 2005). *VizieR Online Data Catalog*, *343*, 81163(3), 1163–1173. https://doi.org/10.1051/0004-6361:20042523

Kirkby, J., Curtius, J., Almeida, J., Dunne, E., Duplissy, J., Ehrhart, S., et al. (2011). Role of sulphuric acid, ammonia and galactic cosmic rays in atmospheric aerosol nucleation. *Nature*, *476*, 429–433. https://doi.org/10.1038/nature10343

Korte, C., Kozur, H. W., & Veizer, J. (2005). [delta]13c and [delta]18o values of Triassic brachiopods and carbonate rocks as proxies for coeval seawater and palaeotemperature. *Palaeogeography, Palaeoclimatology, Palaeoecology*, *226*(3–4), 287–306. https://doi.org/10.1016/j.palaeo.2005.05.018

Krissansen-Totton, J., Buick, R., & Catling, D. (2015). A statistical analysis of the carbon isotope record from the Archean to Phanerozoic and implications for the rise of oxygen. *American Journal of Science*, *315*(4), 275–316. https://doi.org/10.2475/04.2015.01

Kump, L. R., & Arthur, M. A. (1999). Interpreting carbon-isotope excursions: Carbonates and organic matter. *Chemical Geology*, *161*(1), 181–198. https://doi.org/10.1016/S0009-2541(99)00086-8

Lada, C. J., & Lada, E. A. (2003). Embedded clusters in molecular clouds. *Annual Review of Astronomy and Astrophysics*, *41*, 57–115. https://doi.org/10.1146/annurev.astro.41.011802.094844

Large, R. R., Halpin, J. A., Danyushevsky, L. V., Maslennikov, V. V., Bull, S. W., Long, J. A., et al. (2014). Trace element content of sedimentary pyrite as a new proxy for deep-time ocean–atmosphere evolution. *Earth and Planetary Science Letters*, *389*, 209–220. https://doi.org/10.1016/j.epsl.2013.12.020

Large, R. R., Halpin, J. A., Lounejeva, E., Danyushevsky, L. V., Maslennikov, V. V., Gregory, D., et al. (2015). Cycles of nutrient trace elements in the phanerozoic ocean. *Gondwana Research*, *28*(4), 1282–1293. https://doi.org/10.1016/j.gr.2015.06.004

Mermilliod, J.-C. (1993). *Open cluster database*. Retrieved from https://webda.physics.muni.cz

Müller, P., & Suess, E. (1979). Productivity, sedimentation rate, and sedimentary organic matter in the oceans: I. Organic carbon preservation. *Deep-Sea Research*, *26*(12), 1362–1374. https://doi.org/10.1016/0198-0149(79)90003-7

Munz, P. M., Steinke, S., Böll, A., Lückge, A., Groeneveld, J., Kucera, M., & Schulz, H. (2017). Decadal resolution record of Oman upwelling indicates solar forcing of the Indian summer monsoon (9–6ka). *Climate of the Past*, *13* (5), 491–509. https://doi.org/10.5194/cp-13-491-2017

Racki, G. (2005). Chapter 2—Toward understanding late Devonian global events: Few answers, many questions. In D. Over, J. Morrow, & P. Wignall (Eds.), *Understanding late Devonian and Permian-Triassic biotic and climatic events* (Vol. 20, p. 5–36). Elsevier. https://doi.org/10.1016/S0920-5446(05)80002-0

Rich, J. E., Johnson, G. L., Jones, J. E., & Campsie, J. (1986). A significant correlation between fluctuations in seafloor spreading rates and evolutionary pulsations. *Paleoceanography*, *1*(1), 85–95. https://doi.org/10.1029/PA001i001p00085

Rocha-Pinto, H. J., Maciel, W. J., Scalo, J., & Flynn, C. (2000). Chemical enrichment and star formation in the Milky Way disk. II. Star formation history. *Astrophysics*, *358*, 869–885. http://aa.springer.de/papers/0358003/2300869/small.htm

Royer, D. L., Berner, R. A., Montaez, I. P., Tabor, N. J., & Beerling, D. J. (2004). CO_2 as a primary driver of Phanerozoic climate. *Geological Society of America Today*, *14*(3), 4–10. https://www.geosociety.org/gsatoday/archive/14/3/pdf/i1052-5173-14-3-4.pdf

Saltzman, M., & Thomas, E. (2012). Chapter 11—Carbon isotope stratigraphy. In *The geologic time scale* (p. 207–232). https://doi.org/10.1016/b978-0-444-59425-9.00011-1

Saltzman, M. R. (2005). Phosphorus, nitrogen, and the redox evolution of the Paleozoic oceans. *Geology*, *33*, 573–576. https://doi.org/10.1130/G21535.1

Santos, F., Gómez-Gesteira, M., deCastro, M., & Álvarez, I. (2011). Upwelling along the western coast of the iberian peninsula: Dependence of trends on fitting strategy. *Climate Research*, *48*(2/3), 213–218. Retrieved from http://www.jstor.org/stable/24872377

Schidlowski, M. (1988). A 3,800-million-year isotopic record of life from carbon in sedimentary rocks. *Nature*, *333*(6171), 313–318. https://doi.org/10.1038/333313a0

Scotese, C., Song, H., Mills, B., & van der Meer, D. (2021). Phanerozoic paleotemperatures: The earth's changing climate during the last 540 million years. *Earth-Science Reviews*, *215*. Retrieved from https://doi.org/10.1016/j.earscirev.2021.103503

Shaviv, N., & Veizer, J. (2003). Celestial driver of Phanerozoic climate. *Geological Society of America Today*, *13*(7), 4–10. https://www.geosociety.org/gsatoday/archive/13/7/pdf/i1052-5173-13-7-4.pdf

Shaviv, N., & Veizer, J. (2004). CO_2 as a primary driver of phanerozoic climate: Comment. *Geological Society of America Today*, *14*, 18. https://www.geosociety.org/gsatoday/archive/14/7/pdf/gt0407.pdf

Shaviv, N. J. (2002). Cosmic ray diffusion from the galactic spiral arms, iron meteorites, and a possible climatic connection. *Physical Review Letters*, *89*, 051102. https://doi.org/10.1103/PhysRevLett.89.051102

Shaviv, N. J. (2003). The spiral structure of the Milky Way, cosmic rays, and ice age epochs on Earth. *New Astronomy*, *8*, 39–77. https://doi.org/10.1016/S1384-1076(02)00193-8

Shields, G., & Veizer, J. (2002). Precambrian marine carbonate isotope database: Version 1.1. *Geochemistry, Geophysics, Geosystems*, *3*(6). https://doi.org/10.1029/2001GC000266

Sial, A. N., Chen, J., Korte, C., Pandit, M. K., Spangenberg, J. E., Silva-Tamayo, J. C., et al. (2021). Hg isotopes and enhanced hg concentration in the meishan and guryul ravine successions: Proxies for volcanism across the permian-triassic boundary. *Frontiers of Earth Science*, *9*, 477. https://doi.org/10.3389/feart.2021.651224

Sloan, T., & Wolfendale, A. (2013). Cosmic rays and climate change over the past 1000 million years. *New Astronomy*, *25*, 45–49. https://doi.org/10.1016/j.newast.2013.03.008

Smith, A. G., & Pickering, K. T. (2003). Oceanic gateways as a critical factor to initiate icehouse Earth. *Journal of the Geological Society*, *160*(3), 337–340. https://doi.org/10.1144/0016-764902-115

Sun, Y., Joachimski, M. M., Wignall, P. B., Yan, C., Chen, Y., Jiang, H., et al. (2012). Lethally hot temperatures during the early Triassic greenhouse. *Science*, *338*(6105), 366–370. https://doi.org/10.1126/science.1224126

Svensmark, H. (1998). Influence of cosmic rays on earth's climate. *Physical Review Letters*, *81*, 5027–5030. https://doi.org/10.1103/PhysRevLett.81.5027

Svensmark, H. (2006a). Cosmic rays and the biosphere over 4 billion years. *Astronomische Nachrichten*, *327*, 871–875. https://doi.org/10.1002/asna.200610651

Svensmark, H. (2006b). Imprint of Galactic dynamics on Earth's climate. *Astronomische Nachrichten*, *327*, 866. https://doi.org/10.1002/asna.200610650

Svensmark, H. (2012). Evidence of nearby supernovae affecting life on Earth. *MNRAS*, *423*, 1234–1253. https://doi.org/10.1111/j.1365-2966.2012.20953.x

Svensmark, H., Enghoff, M. B., & Pedersen, J. O. P. (2013). Response of cloud condensation nuclei (> 50 nm) to changes in ion-nucleation. *Physics Letters A*, *377*, 2343–2347. https://doi.org/10.1016/j.physleta.2013.07.004

Svensmark, H., Enghoff, M. B., Shaviv, N. J., & Svensmark, J. (2017). Increased ionization supports growth of aerosols into cloud condensation nuclei. *Nature Communications*, *8*(1), 2199. https://doi.org/10.1038/s41467-017-02082-2

Svensmark, H., & Friis-Christensen, E. (1997). Variation of cosmic ray flux and global cloud coverage – A missing link in solar-climate relationships. *Journal of Atmospheric and Terrestrial Physics*, *59*, 1225–1232.

Svensmark, H., Pedersen, J. O. P., Marsh, N. D., Enghoff, M. B., & Uggerhøj, U. I. (2007). Experimental evidence for the role of ions in particle nucleation under atmospheric conditions. *Proceedings of the Royal Society of London. Series A, Mathematical and Physical Sciences*, *463*, 385–396. https://doi.org/10.1098/rspa.2006.1773

Svensmark, H., Svensmark, J., Enghoff, M. B., & Shaviv, N. J. (2021). Atmospheric ionization and cloud radiative forcing. *Scientific Reports*, *11*(1), 19668. https://doi.org/10.1038/s41598-021-99033-1

Svensmark, J., Enghoff, M. B., Shaviv, N. J., & Svensmark, H. (2016). The response of clouds and aerosols to cosmic ray decreases. *Journal of Geophysical Research: Space Physics*, 8152–8181. https://doi.org/10.1002/2016JA022689

Walliser, O. H. (1996). Global events in the Devonian and carboniferous. In O. H. Walliser (Ed.), *Global events and event stratigraphy in the phanerozoic: Results of the international interdisciplinary cooperation in the IGCP-project 216 "global biological events in earth history"* (pp. 225–250). Springer Berlin Heidelberg. https://doi.org/10.1007/978-3-642-79634-0_11

Werner, M., Kissmann, R., Strong, A., & Reimer, O. (2015). Spiral arms as cosmic ray source distributions. *Astroparticle Physics*, *64*, 18–33. https://doi.org/10.1016/j.astropartphys.2014.10.005

Zeebe, R. E. (1999). An explanation of the effect of seawater carbonate concentration on foraminiferal oxygen isotopes. *Geochimica et Cosmochimica Acta*, *63*(13–14), 2001–2007. https://doi.org/10.1016/S0016-7037(99)00091-5

Zeebe, R. E. (2001). Seawater ph and isotopic paleotemperatures of cretaceous oceans. *Palaeogeography, Palaeoclimatology, Palaeoecology*, *170*(1–2), 49–57. https://doi.org/10.1016/S0031-0182(01)00226-7